Mitig Adapt Strateg Glob Change
DOI 10.1007/s11027-013-9490-y

ORIGINAL ARTICLE

A satellite-based disturbance index algorithm for monitoring mitigation strategies effects on desertification change in an arid environment

Nasem Badreldin · Rudi Goossens

Received: 20 April 2013 / Accepted: 4 July 2013

Abstract This research focuses on monitoring the desertification change as a result of mitigation and adaptation strategies in arid environmental condition. Exploring environmental hazards, specifically desertification development, is important for understanding loss of productivity in dry lands. Developing a new satellite-based algorithm for monitoring desertification in an arid environment delivers information useful in protecting the environment and mitigating natural hazards. A multi-temporal remote sensing data of MODerate resolution Imaging Spectroradiometer (MODIS) were used for estimating the Soil-Adjusted Vegetation Index (SAVI) and Land Surface Temperature (LST), based on monthly data during the years 2002, 2005, 2008 and 2011. The MODIS-based disturbance index (MBDI) was improved by estimating the long-term variation in the ratio of annual maximum composite LST and SAVI on a pixel-by-pixel basis. A significant correlation (r=−0.88; P<0.001) was found between the mean-maximum SAVI and mean-maximum LST in the dry season. The response of the MBDI to land degradation was assessed by comparing the obtained soil salinity data to the algorithm outcomes. The results showed that the proposed new satellite-based algorithm has a high potential to detect the spatial extent of prime land degradation in an arid environment. Also, this algorithm was able to recognize the difference between the natural variability and instantaneous/non-instantaneous desertification symptoms in an arid environment. The mitigation strategies in the case study decreased the desertification development and combat the land degradation in the last decade.

Keywords MODIS-based disturbance index algorithm · Desertification · Remote sensing · Mitigation strategies effects · Sinai Peninsula

1 Introduction

Deserts around the world share common characteristics in terms of their edaphic environments, climate, geomorphology, and hydrology (Laity 2008). The wildlife adapted their morphology formation and metabolism to conserve moisture and avoid effects of

N. Badreldin (✉) · R. Goossens
Department of Geography, Ghent University, Krijgslaan 281 S8, 9000 Ghent, Belgium
e-mail: nasem.badreldin@ugent.be

Published online: 20 July 2013

aridity (Harris 2003). Deserts have become the new home for agriculture and business for 900 million people (Thomas 2011), resulting in a need for smart and innovative desert management solutions. Such solutions will require the monitoring of hazards and natural resources.

Desertification is one of the hazards that face arid environments, which is the process whereby the productivity of land is reduced, this land deterioration involves changes in vegetation cover by reduction, replacement, and destruction (Kassas 1977). Desertification plays a vital role in land cover distribution in arid regions. While incidents of drought prevail in all climate zones of the world, the impacts of drought are deeply felt in drier lands (Diouf and Lambin 2001; Grainger et al. 2000; Kassas 1995; Stiles 1984). Desertification directly affects about one-fifth of the world population in over 110 developing countries (Adamo and Crews-Meyer 2006; Armah et al. 2010; Kepner et al. 2006). According to the interpretation of the United Nations Convention to Combat Desertification (UNCCD) definition of desertification, estimating environmental disturbance can be used as an indicator to determine desertification change (Dawelbait and Morari 2012; Salinas and Mendieta 2012b). Disturbance has been defined as any factor that brings significant changes to the ecosystem over more than 1 year, and that occurs over large spatial scales (Pickett and White 1987; Tilman 1985).

Climate change increases the desertification threat (Salinas and Mendieta 2012c). Agricultural activity is highly related to the interaction between the socioeconomic and environmental situations. The efficient use of natural resources in arid environment is a vital strategy to combat the climate change and desertification effects (Misra 2013; Salinas and Mendieta 2012a). Monitoring disturbances in arid eco-systems is essential, especially in agro-ecosystems affected by desertification, in order to manage food security by improving agriculture and promoting sustainable mitigation strategies as anti-desertification act (Armah et al. 2010).

Remotely sensed data provide multi-temporal information that reflects environmental changes in the Earth's surface (Bannari et al. 1995; Hall et al. 1995; Herrmann et al. 2005; Richards 2013; Wang et al. 2008). Integration with geographic information systems (GIS) offers a wide range of facilities for better data analysis and interpretation (Weng 2002).

In this investigation, we propose a new satellite-based disturbance index algorithm for monitoring ago-ecosystem changes in arid environmental conditions in the years 2002, 2005, 2008 and 2011. We will also assess the relationship between the land surface temperature and vegetation cover at different sites in the Sinai Peninsula Egypt, thereby providing useful information about biophysical feedback.

2 Materials and methods

2.1 Study area description and field survey

The total area of the Sinai Peninsula is 61,000 km^2, and it occupied about 6 % of the total area in Egypt as shown in Fig. 1. The population is almost 500,000, and the majority found in the north of Sinai. (WFP 2006) reported that Sinai remain food insecure and has the highest levels of poverty in Egypt. The main limitation of natural resources in Sinai is water, and there is only marginal capacity for expansion (FAO 2005).

A general overview of Sinai's land use is categorized in five physiographic regions (Dames and Moore 1981). The Mediterranean foreshore is the most inhabited area in the Sinai Peninsula, highly developed in agriculture production, especially El Arish and Raffa,

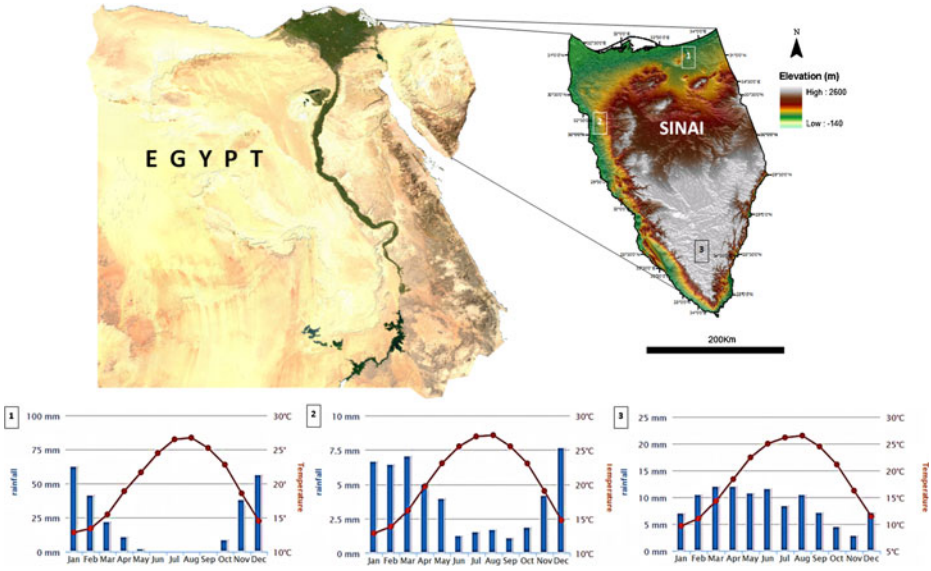

Fig. 1 The geographical location and geomorphology of Sinai Peninsula. Climatic information (*lower section*), presenting the mean rainfall and air temperature of period (1980: 2012) for different locations over the case study, rainfall (*blue columns*) and air temperature (*red lines*)

see Table 1. The greatest environmental threats in North Sinai are shifting sand dunes and soil salinity; fishing provides a major form of nourishment along the coast and El-Bardawil Lake. The regions of mobile and stable platforms are sparsely inhabited, agriculture activity is restricted to rain-fed patches in the wadi beds, and urbanization growth is stunted because of the considerable distance from markets and shipping. Suez Rift Province, on the western coastline, is relatively well populated, the growth of agriculture is gradual because of the lack of a reliable source of fresh water, industrial capacity is substantial, based on the potential for extracting mineral and petroleum resources; it also has a strong potential for development of tourism. Southern Mountains Province is extremely sparsely inhabited, agriculture is always near oases, and there is poor grazing. The future land use in the Southern Mountains Province will almost entirely be limited to tourism.

Table 1 The most common vegetation types (crops and flora) in Sinai Peninsula, based on field survey and statistical data of (North Sinai Governorate 2011)

Vegetation category	Types
Irrigated crops	Olives (*Olea europaea*), Pomegranates (*Punica granatum*), Almonds (*Prunus amygdalus*), Oranges (*Citrus sinensis*), Lemons (*Citrus limon*), and Figs (*Ficus carica*) Tomatoes (*Solanum lycopersicum*), Cucumbers (*Cucumis sativus*), Bell pepper (*Capsicum annuum*), Eggplant (*Solanum melongena*), Watermelon (*Citrullus lanatus*), and Okra (*Abelmoschus esculentus*)
Non-irrigated crops	Barley (*Hordeum vulgare*), wheat (*Triticum aestivum*) and Date Palm (*Phoenix dactylifera*)
Natural plants	Glaucous Glasswort (*Arthrocnemum glaucum*), Somerset Rush (*Juncus subulatus*), White Bean-Caper (*Zygophyllum album*), and Athel tree (*Tamarix aphylla*)

Based on the classification system (soil taxonomy) that was developed by the United States Soil Conservation Services (USSCS), the major soil groups that have been found in Sinai are Entisols and Aridisols (Greenwood 1997). Natural Resources Conservation Service, NRCS (1999) described the soils that are found in the Entisols order as having little or no development of pedogenic horizons, and some of these soils are on a site that is actively eroding or are found in additional deposits (alluvium, in the wadis or aeolian, forming sand dunes). Original soils in this category, which occupy most of North Sinai, consist mainly of quartz or other minerals that are resistant to the weathering needed to develop diagnostic horizons. The Aridisols order represents the soils that developed in a stable arid environment setting, where water has not been available to mesophytic plants for a long time, this order was found in the middle and south of Sinai, in places such as El-Tih plateau, where it was classified to the Orthid suborder and soil group of Typic Calciorthids, which contain calcic horizons with accumulation of≥15 % calcium carbonate.

Kottek et al. (2006) and Peel et al. (2007) updated the climate classification of Köppen-Geiger, and Sinai was classified as (Bwh) arid-desert-hot climate, where the southern part of Sinai is more dry and more arid than the north, the south received less rain in the winter <5 mm a year and air temperature is between 10–20 °C in the winter and 30–40 °C in the summer. The north is less dry, rainfall is <200 mm and 5–20 °C in winter and air temperature 20–35 °C (World Bank 2013).

Six study sites were chosen to represent the variety of the land cover of the Sinai Peninsula; a field survey was conducted to observe land cover types in different arid environmental conditions. Also, anthropological activities were different in terms of agricultural management and urbanization growth, which were influencing the agro-ecosystem distribution. Ten soil samples were collected based on a random sampling design (unbiasedness) and representativeness for each study site in order to analyze physical soil properties along with the field observations as shown in Table 2.

Table 2 Description of soil properties and filed survey observations for six chosen study sites in Sinai Peninsula

Location	Latitude	Longitude	Description
El-Tina Plain,	31° 00′ 00.09″	32° 26′ 11.25″	Soil contains fine particles size, elevation < 50 m, waterlogging and salinization is the major land degradation. Cultivation is the main agricultural activity, plant cultivars are mostly salt tolerant
Arish&Rafaa	31° 09′ 35.72″	34° 02′ 11.83″	Soil contains coarse to moderate particle sizes, elevation < 150 m, wind erosion in the major land degradation, cultivation and natural plant are the major characteristic of vegetation cover.
Qantara Shark	30° 26′ 31.58″	32° 24′ 23.19″	Soil contains coarse particle sizes, elevation < 100 m, wind erosion and sandstorms are the major land degradation, intensive agricultural production and various plant cultivars.
Zaraniq	31° 06′ 07.77″	33° 28′ 57.82″	Soil contains coarse particle sizes, elevation < 50 m, wind erosion and salinization are the major land degradation, natural halophyte plant species.
South-Sinai	28° 27′ 38.70″	34° 04′ 15.03″	Soil contains coarse particle sizes, elevation > 2,000 m, water erosion is the major land degradation, drought tolerant natural plants species.
El-Wasat	29° 52′ 08.36″	33° 47′ 21.85″	Soil contains moderate to fine particle sizes, elevation < 1,500 m, water erosion is the major land degradation, drought tolerant natural plants species and rare cultivation activity.

2.2 Statistical analysis

The spatial pixel-based scale of the data was considered in the analysis; the polygons correspond to the territorial disparities in the vegetation cover along the land surface temperature. The relationship between maximum land surface temperature (LST) and maximum soil-adjusted vegetation index (SAVI) across different sites in the study area was estimated using land cover types that were explored during field work in 2011. The mean-maximum LST and SAVI were calculated as the sum of the highest values at each location for the studied periods within the observed land cover types. To assess the significance of the relationship between SAVI and LST on the regional scale, Pearson's correlation analysis (r) was used, and the confidence limits surrounding r were calculated (Zahran and Willis 2009; Zar 2010).

2.3 Remote sensing data

This study was based on MODerate resolution Imaging Spectroradiometer (MODIS) satellite images, which were obtained from the Earth Resources Observation and Science (EROS) Center. Monthly data in the years 2002, 2005, 2008 and 2011 in clear atmospheric conditions were acquired for this study. MODIS Re-projection Tool (MRT) software version 4.1 was used to reproject MODIS images into a known map projection system and extension. The MOD13A3 satellite is the MODIS Terra, vegetation indices (VI) were provided monthly at 1 km spatial resolution and used for estimating SAVI, VI were computed from atmospherically corrected bi-directional surface reflectance's that were masked for water, clouds, heavy aerosols, and cloud shadows (U.S. Geological Survey 2011a). The MOD09Q1 satellite is the MODIS Terra, LST was provided every 8 days of data at 250 m spatial resolution, the data were validated via a widely distributed dataset of locations and time periods via several ground-truths and were ready for use in scientific publications (U.S. Geological Survey 2011b). Global Multi-resolution Terrain Elevation Data 2010 (GMTED2010) provided a new level of detail in global topographic data, the accuracy was measured by a global set of control points, root mean square error (RMSE) of the products that were used for this study was between 26 and 30 m at 7.5 arc-seconds (U.S. Geological Survey 2011c).

2.4 MBDI improvement for monitoring desertification change

The MODIS-based disturbance index (MBDI) is the ratio of annual maximum composite LST and SAVI. Based on a multi-temporal datasets, it is designed to capture long-term variations on a pixel-by-pixel basis, and to detect significant inter-annual changes in surface energy, which is responsible for the natural variability of instantaneous and non-instantaneous desertification symptoms (e.g., erosion, overgrazing, climate change and drought) (Mildrexler et al. 2007).

$$MBDI_i = \frac{\frac{LST_{i\ max}}{SAVI_{i\ max}}}{\sum_{i-1}\left(\frac{LST_{max}}{SAVI_{max}}\right)} \tag{1}$$

Where $MBDI_i$ is the MBDI value for year i, $LST_{i\ max}$ is the annual maximum 8-day composite LST for year i, $SAVI_{i\ max}$ is the annual maximum 16-day SAVI for year i, LST_{max}

is the multiyear LST_{max} but, not including the analysis year (i−1) and $SAVI_{max}$ is the multiyear mean of $SAVI_{max}$ but not including the analysis year (i−1).

The VI values were affected by the reflectance of light in the red and near-infrared spectra, where the vegetative cover was lower than 40 %, and the soil surface was exposed, which is a typical environment in arid regions (Yang et al. 2012). In order to correct the influence of the ground brightness when vegetative cover is low, the NDVI was modified through SAVI (Bannari et al. 1995; Huete 1988).

$$SAVI = \left(\frac{\rho_{NIR} - \rho_{RED}}{\rho_{NIR} + \rho_{RED} + L}\right) \times (1 + L) \quad (2)$$

Where ρ_{NIR} is the reflectance value of the near infrared band, ρ_{RED} is the reflectance of the red band, and L is the soil brightness correction factor. L=0.5 was successfully minimizing the impact of soil variations in green vegetation compared to NDVI (Aboelghar et al. 2012).

According to (Coops et al. 2009; Mildrexler et al. 2007) the success of this algorithm was dependent on two factors: (1) sufficiently strong and frequent signals to detect disturbance and (2) having signals greater than the natural variability. The disturbance in Sinai occurred as a result of vegetation demise, which will lead to an increase in LST.

The natural variability was defined for each individual pixel that falls within ± standard deviation for the long-term mean LST/SAVI ratio. Instantaneous disturbance such as water erosion and floods cause an immediate increase in MBDI from the natural variability range, whereas non-instantaneous disturbance such as drought and soil salinization, will incrementally shift the MBDI from the natural variability range, and may be recovered in the long or short term, depending on mitigation and remediation programs and methods, see Fig. 2.

The development of desertification was observed in many regions in Sinai, the bi-stable ecosystem dynamics, as shown in Fig. 3, can explain the desertification development in the case study. Both vegetated and desertified states are the stable configurations of the system (D'Odorico et al. 2013). A disturbance can cause a transition to the stable states, and the resilience to change

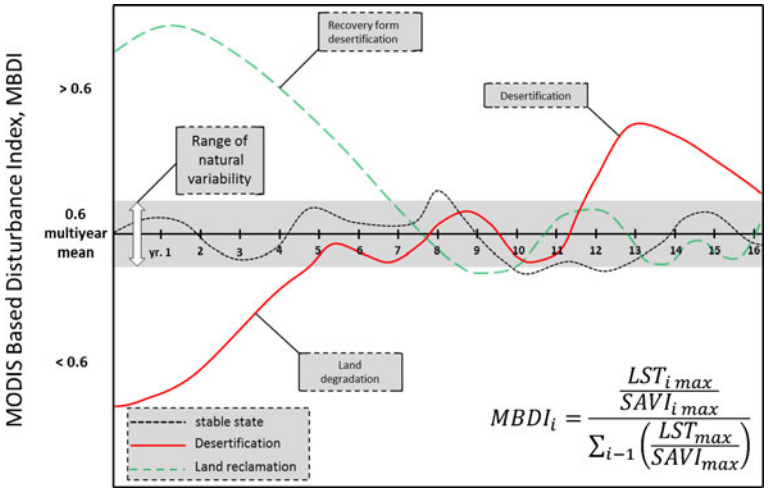

Fig. 2 The MODIS Based Disturbance Index (MBDI) algorithm with a bi-directional aspect, for tracking the disturbance that caused by desertification in an arid environment. The normal environmental condition exist in the range of the natural variability (*gray zone*), when the studied year LST_{max} and $SAVI_{max}$values has the mean of 0.6. In cases of desertification the LST_{max} increases and the $SAVI_{max}$ decreases (*red solid line*). The recovery state found when the LST_{max} decreases and the $SAVI_{max}$ increases (*green dashed line*)

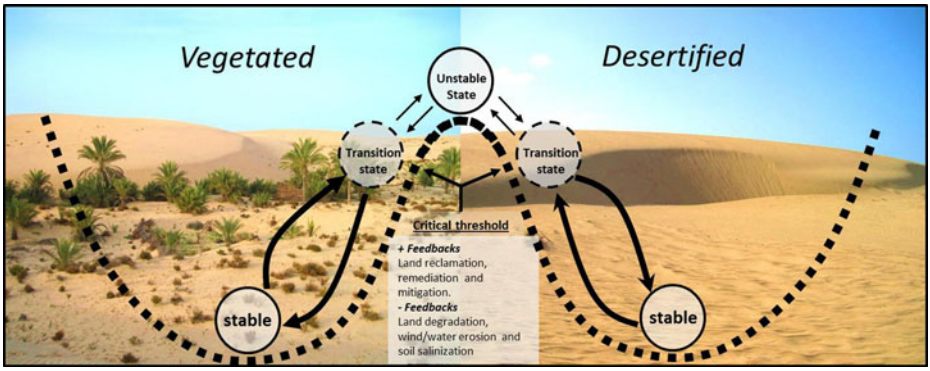

Fig. 3 Illustration draws of the bi-stable ecosystem balance for an arid environment, both sections (vegetated and desertified) are hosting the transition and stable states, the critical threshold containing (positive and negative) environmental feedbacks. Positive feedbacks are the drivers that influence the system positively to move to the vegetated section, where the negative feedbacks are the drivers that cause more land degradation and orient the system to move to the desertified section

of the bi-stable system depends on the disturbance strength per duration; if the system makes a transition to the other stable state it will be difficult to revert to the initial state (Gunderson 2000).

2.5 Assessing the MBDI algorithm

Many disturbance agents such as sand dunes shifting, flash flood, and over grazing were attributed to MBDI change in the case study, but the soil salinity was considered the greatest land degradation in Sinai (Nawar et al. 2011). The salt accumulation occurred as a result of evaporation to the salty waterlogging, which formed salt crust on the soil surface (Carrow and Duncan 2012). The soil salinity in the case study was classified into five groups as shown in Table 3. And 44 soil samples were collected from different spots in north Sinai for analyzing soil salinity using the

Table 3 The classification of soil salinity and field observation for each class, based on the soil salinity classification and EC ranges (Carrow and Duncan 2012)

Soil salinity type	EC range (dS/m)	Field observation
Non-saline	<2	▪ No salt crust or affected vegetation by soil salinity. ▪ Intensive agricultural activities and fruit production. ▪ No observations of waterlogging areas or saline soils "Sabkhas".
Slightly-saline	2–4	▪ Salt tolerant species found in healthy condition. ▪ Land cultivation and drip irrigation system. ▪ No observations of surface salt crystals.
Moderately-saline	4–8	▪ Domination of salt tolerant natural plants community. ▪ No cultivation areas and more land reclamation activities. ▪ Present of small bare areas and salt with salt crusts.
Highly-saline	8–16	▪ Domination of salt tolerant natural plants community. ▪ No cultivation areas and more land reclamation activities. ▪ Large bare saline areas and wetlands as a result of the uprising waterlogging.
Extremely-saline	>16	▪ Domination of the halophyte species and dead natural plants. ▪ Salt mining activities for industrial production. ▪ Large white land surface as a result of salt crust accumulation.

saturated paste extraction method (U.S. Salinity Laboratory 1954). The obtained data from the field were compared with the number of MBDI pixels, that were disturbed over the same temporal-frame (2011) and spatial location, as shown in Fig. 4. The results showed a strong relationship between the measured data (soil samples) and the estimated values of disturbance (MBDI) (r=0.79; p<0.001), which approved using the algorithm for monitoring the desertification in the case study.

3 Results and discussions

3.1 Mean-maximum LST and SAVI relationship

The mean-maximum SAVI and mean-maximum LST over Sinai for 2011 were negatively correlated (r=−0.88; P<0.001) after the dry season in the case study (September), see Fig. 5. The land cover types in the case study were observed during field work, and connected to the modified energy balance curve in Fig. 5 according to the hypothesized groups by (Mildrexler et al. 2007; Nemani and Running 1997). In the water-limited section, plant communities grow in drier weather or poor soil conditions, also the high fraction of the exposed soil increases the LST as a result of inadequate water supply. The predominant land cover types for this section were barren lands and desert flora (Fig. 6a, b), where LST was high and SAVI low. In the energy-limited section, wetlands and open water fall into this category, the water adequacy is responsible for low LST and Bowen ratios, the dominant land cover types that were found in this section were wetlands "Sabkhas" and halophyte species, which were tolerant to salty water conditions (Fig. 6c). the atmospherically decoupled section has a distinctive vegetation cover type different to the ecological optimality as a result of agricultural activity, which provided fertilization and appropriate irrigation systems for a dry environment, such as sprinkler and drip irrigation regimes for maximum vegetation production in high LST. Crops were the dominant land

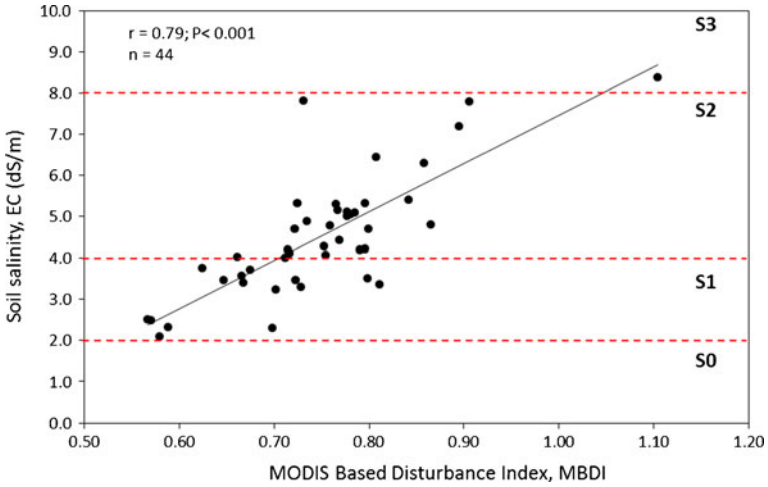

Fig. 4 Soil salinity, EC (dS/m) and the MODIS-Based Disturbance Index, MBDI relationship; n=44 soil samples were obtained during field survey in 2011, the soil salinity classified into four major groups, see Table 3. **S0:** Non-saline (< 2 dS/m); **S1:** Slightly-saline (2–4 dS/m); **S2:** Moderately-saline (4–8 dS/m); **S3:** Highly-saline (8–16 dS/m)

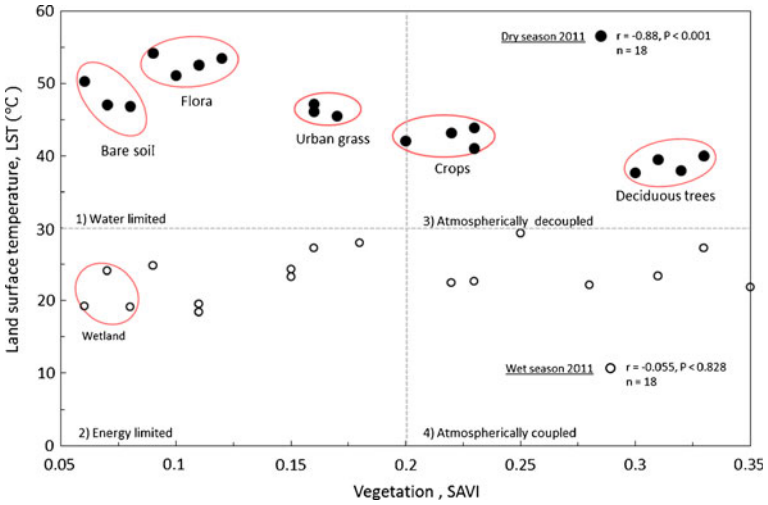

Fig. 5 The distribution of land cover types in Sinai Peninsula based on the energy balance relationship, over four environmental categories, which are conceptualized by (Nemani and Running 1997)

cover type found during the field work, as shown in Fig. 6d. The climate and soil properties controlled the vegetation density in the atmospherically coupled section, trees with deep-root systems tend to dissipate more energy by transpiration through much of the growing season, this land cover type has high vegetation cover and low exposed ground, which was responsible for the low radiometric temperature, Fig. 6e.

The relationship between mean-maximum LST and maximum SAVI across the Sinai Peninsula at each pixel for the years 2002, 2005, 2008 and 2011 provided useful information to determine the spatial variation of disturbance. Six sites were chosen with different characteristics, in order to represent the whole Sinai Peninsula. This relationship across Sinai provided an initial assessment of the vegetation cover variation over the studied years as shown in Fig. 7. Arish&Rafaa and Qantara Shark sites, dominated by agriculture (Badreldin and Goossens 2013), and after the year 2002 El-Tina Plain became a zone for crop production as a result of El-Salam Canal project for land reclamation and agricultural production (Othman et al. 2012). As shown in Fig. 7a, b and c. Zaraniq, South-Sinai and El-Wasat have constant low SAVI over different LSTs, which varied from 50 °C in the summer seasons such as June and September, to approximately 15 °C in January and December. As shown in Fig. 7d, e and f, these sites were dominated by natural plants that have tolerance to arid environmental conditions.

In general, the increase in LST in the case study was associated with strong evaporation and water logging that carried the soluble salts up to the soil surface (Ci and Yang 2009), salt accumulates on soil surface as a salt crust and affects agricultural production and ecosystems stability, and permanently degrades soil productivity (Rengasamy 2006).

3.2 MBDI application for desertification recovery detection

We applied the MBDI algorithm to the MODIS data for the years 2002, 2005, 2008 and 2011 across the Sinai Peninsula. The mean MBDI value for the entire study area was 0.6. The MBDI range was extended from <0.5 to >1.2. The natural variability range was defined as the values that found within one standard deviation ±0.1 of the mean 0.6. The natural

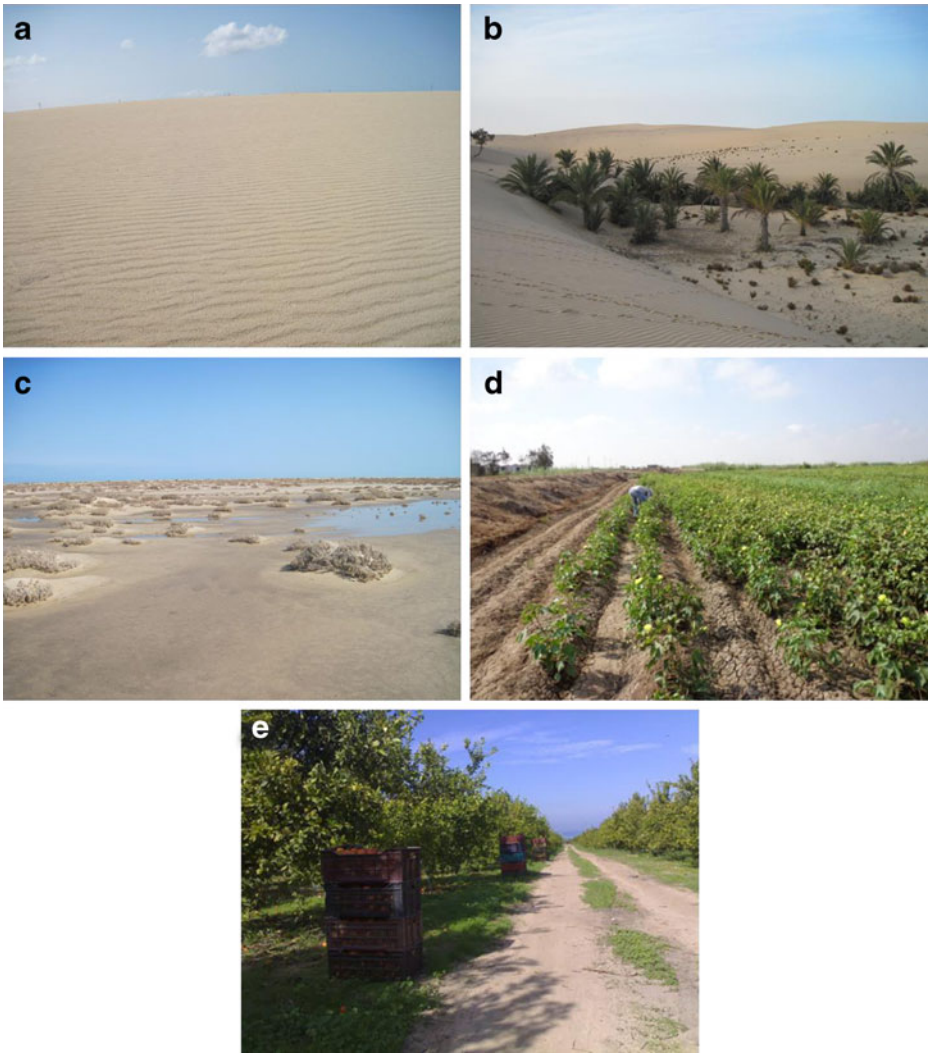

Fig. 6 Different examples of land cover classes in Sinai Peninsula; **a** barren lands ; **b** natural plants; **c** wetlands "sabkhas"; **d** crops, taken by Said Nawar; **e** deciduous trees, taken by Abo Al-Amer

variability range 0.7–0.5 was mapped in yellow, moderate disturbance 0.7–1.2 was mapped in orange, extreme disturbance values >1.2 in red, and <0.5 for the recovery was mapped in gray. The MBDI algorithm detected a recovery from desertification at sites in El-Tina plain and Qanatra Shark, through the studied years 2002, 2005, 2008 and 2011.

The soil properties in the El-Tina Plain area are a combination of alluvium deposits, originating from ancient Nile River branches, and lacustrine sand deposits (Hassan 2002), which covered the north-western corner of Sinai. (Nawar et al. 2011) classified the salt-affected soils in the El-Tina plain as very strong saline soils >32 $dS.m^{-1}$, strongly saline soils 16–32 $dS.m^{-1}$, moderately saline soils 8–16 $dS.m^{-1}$, slightly saline soils 4–8 $dS.m^{-1}$, and very slightly saline 2–4 $dS.m^{-1}$. The southern part of the El-Tina plain recovered from

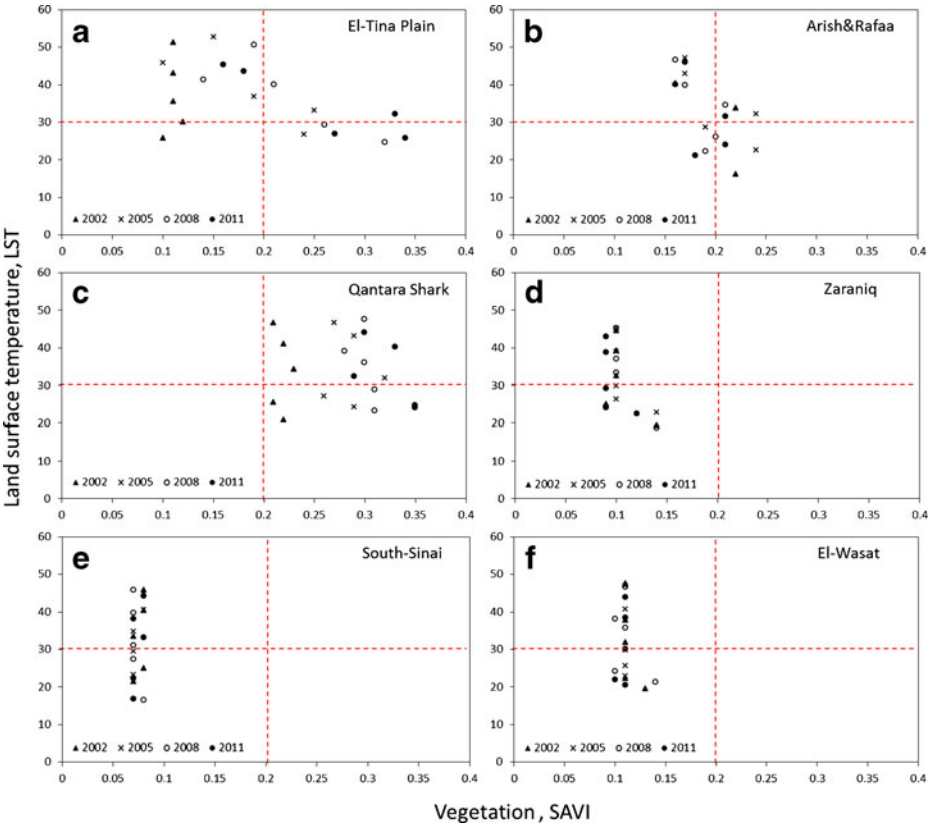

Fig. 7 The mean-maximum LST and SAVI relationship over years 2002, 2005, 2008 and 2011; **a** El-Tina Plain, Lat. 31° 00′ 00.09″, Long. 32° 26′ 11.25″; **b** Arish&Rafaa, Lat. 31° 09′ 35.72″ Long. 34° 02′ 11.83″; **c** Qantara Shark, Lat. 30° 26′ 31.58″, Long.32° 24′ 23.19″; **d** Zaraniq, Lat. 31° 06′ 07.77″, Long. 33° 28′ 57.82″; **e** South Sinai, Lat. 28° 27′ 38.70″, Long. 34° 04′ 15.03″; **f** El-Wasat, Lat. 29° 52′ 08.36″, Long. 33° 47′ 21.85″

desertification over the years 2002, 2005, 2008 and 2011, as shown in Fig. 8a, as a result of extensive agricultural development, (Kaiser 2009) found that the cultivated land areas increased significantly while wetlands decreased over the years.

Wind erosion in the north of Sinai is considered one of the earth's surface dynamics that impacts infrastructure and farming activities via sand dunes shifting. The ecosystem in Qantara Shark is affected by sand dunes' progress at different rates and directions (Hermas et al. 2012). As shown in Fig. 8b, the societal feedbacks contributed through the years 2002, 2005, 2008 and 2011 against the desertification, and the spatial distribution of the desertification (MBDI >1.2 and 0.7–1.2) decreased in the years 2005, 2008 and 2011, which indicated that the environment in this site is improving.

MBDI detected evidences of mitigation investments which decreased desertification and land degradation in the case study. Soil leaching was the strategy for decreasing the salinity in order to improve the physical and chemical soil properties for agriculture production, which was given a high national priority (Galal 2004). Also, planting windbreaks to decrease the wind erosion effects in Qantara Shark has a significant impact to improve the agriculture activity and to minimize the soil erodibility.

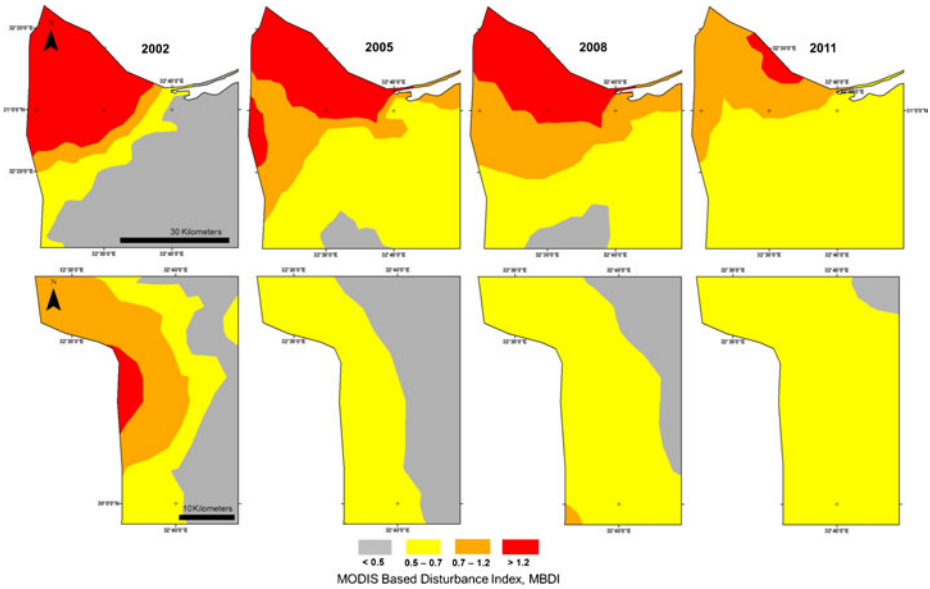

Fig. 8 The MBDI spatial distribution over the years 2002, 2005, 2008 and 2011; **a** El-Tina Plain; **b** Qanatra Shark. Disturbance recovery is < 0.5 (*gray color*), the natural variability range is between 0.5–0.7 (*yellow color*), moderate disturbance 0.7–1.2 (*orange color*), and extreme disturbance is > 1.2 (*red color*)

4 Conclusion

MBDI algorithm was developed for monitoring the desertification status in an arid environment for regional scales, and based on Aqua/MODIS and Terra/MODIS satellites. This algorithm proved to be a useful method for disturbance detection. The advantages of using MBDI were to provide accurate change detection information about the spatial and temporal departure of disturbance events, and its recovery in arid ecosystems regarding to its natural condition. Mean-maximum LST and SAVI relationship was considered at two different seasons, 1) the most vulnerable biotic condition, when the vegetated areas undisturbed, and 2) the abiotic environment. The relationship between maximum LST and maximum SAVI across different sites in the study area were strongly negatively correlated (r=−0.88; P<0.001) after the dry season in September. Classes of MBDI were defined for the natural variability, extreme disturbance, moderate disturbance and recovery status (0.5–0.7, >1.2, 0.7–0.5 and <0.5, respectively). MBDI detected anti-desertification change in El-Tina plain and Qanatra Shark through over the studied years 2002, 2005, 2008 and 2011. Soil salinization and wind erosion were the main land degradation that desertified lands in Sinai Peninsula. Societal drivers in El-Tina plain and Qanatra Shark sites contribute to mitigate and compact desertification process, some of soil remediation practices such soil leaching enhanced salt accumulation in the shallow soils of El-Tina plain.

MBDI provided a powerful tool for monitoring positive and negative changes of desertification in an arid environment in regional level. Also, it can be used for detecting and predicting the effects of the climate change, and deliver accurate information about the environmental risk assessment or the early warning system for decision makers, organizations and public awareness, in order to prevent severe desertification and land degradation events and protect the local natural resources and biodiversity.

Acknowledgments This research was supported by Agricultural Research and Development Fund (ARDF) in Egypt. We gratefully acknowledge U.S. National Aeronautics and Space Administration (NASA) and Earth Observing System (EOS) for the data support. We thank Dr. Constance Ellwood, Mrs. Christina Thomas and ir. Ali Youssef for their valuable suggestions, and the anonymous reviewers for their criticism that improved the manuscript.

References

Aboelghar M, Ali A-R, Arafat S (2012) Spectral wheat yield prediction modeling using SPOT satellite imagery and leaf area index. Arab J Geosci. doi:10.1007/s12517-012-0772-6

Adamo SB, Crews-Meyer KA (2006) Aridity and desertification: exploring environmental hazards in Jáchal, Argentina. Appl Geogr 26:61–85

Armah FA, Odoi JO, Yengoh GT et al (2010) Food security and climate change in drought-sensitive savanna zones of Ghana. Mitig Adapt Strateg Glob Chang 16:291–306

Badreldin N, Goossens R (2013) Monitoring land use/land cover change using multi-temporal Landsat satellite images in an arid environment: a case study of El-Arish, Egypt. Arab J Geosci. doi:10.1007/s12517-013-0916-3

Bannari A, Morin D, Bonn F, Huete AR (1995) A review of vegetation indices. Remote Sens Rev 13:95–120

Carrow RN, Duncan RR (2012) Best management practices for saline and sodic turfgrass soils: assessment and reclamation. CRC Press, Taylor & Francis Group, FL, p 486

Ci L, Yang X (2009) Desertification and its control in China. Higher Education Press and Springer, Beijing and Dordrecht, p 533

Coops NC, Wulder MA, Iwanicka D (2009) Large area monitoring with a MODIS-based Disturbance Index (DI) sensitive to annual and seasonal variations. Remote Sens Environ 113:1250–1261

Dames, Moore (1981) Sinai development study—phase 1: land classification and capability in Sinai. 167

Dawelbait M, Morari F (2012) Monitoring desertification in a Savannah region in Sudan using Landsat images and spectral mixture analysis. J Arid Environ 80:45–55

Diouf A, Lambin EF (2001) Monitoring land-cover changes in semi-arid regions: remote sensing data and field observations in the Ferlo, Senegal. J Arid Environ 48:129–148

D'Odorico P, Bhattachan A, Davis KF et al (2013) Global desertification: drivers and feedbacks. Adv Water Resour 51:326–344

FAO (2005) Fertilizer use by crop in Egypt, land and plant nutrition management service land and water development division. Rome, p 62

Galal ME (2004) Estimating soil hydraulic parameters in El-Tina plain using RETC program. International Conf. on Water Resources & Arid Environment. p 5

Grainger A, Smith MS, Squires VR, Glenn EP (2000) Desertification and climate change: the case for greater convergence. Mitig Adapt Strateg Glob Chang 5:361–377

Greenwood NH (1997) The Sinai: a physical geography. University of Texas Press, Austin, p 148

Gunderson LH (2000) Ecological resilience—in theory and application. Annu Rev Ecol Syst 31:425–439. doi:10.1146/annurev.ecolsys.31.1.425

Hall FG, Townshend JR, Engman ET (1995) Status of remote sensing algorithms for estimation of land surface state parameters. Remote Sens Environ 51:138–156

Harris N (2003) Atlas of the world's deserts. Taylor and Francis, New York, p 359

Hassan MAE-RAE-A (2002) Environmental studies on coastal zone soils of the north Sinai peninsula (Egypt) using remote sensing techniques. Technischen Universität Carolo-Wilhelmina, p 247

Hermas E, Leprince S, El-Magd IA (2012) Retrieving sand dune movements using sub-pixel correlation of multi-temporal optical remote sensing imagery, northwest Sinai Peninsula, Egypt. Remote Sens Environ 121:51–60

Herrmann SM, Anyamba A, Tucker CJ (2005) Recent trends in vegetation dynamics in the African Sahel and their relationship to climate. Global Environ Chang 15:394–404

Huete A (1988) A soil-adjusted vegetation index (SAVI). Remote Sens Environ 25:295–309

Kaiser MF (2009) Environmental changes, remote sensing, and infrastructure development: the case of Egypt's East Port Said harbour. Appl Geogr 29:280–288

Kassas M (1977) Arid and semi-arid lands: problems and prospects. Agro-Ecosystems 3:185–204

Kassas M (1995) Desertification: a general review. J Arid Environ 30:115–128

Kepner WG, Rubio JL, Mouat DA, Pedrazzini F (2006) Desertification in the Mediterranean Region. A Security Issue. Proceedings of the NATO Mediterranean Dialogue Workshop on Desertification in the Mediterranean Region. A Security Issue. Springer, Dordrecht, p 606

Kottek M, Grieser J, Beck C et al (2006) World Map of the Köppen-Geiger climate classification updated. Meteorol Z 15:259–263

Laity J (2008) Deserts and desert environments. Wiley, Chichester, p 357
Mildrexler DJ, Zhao M, Heinsch FA, Running SW (2007) A new satellite-based methodology for continental-scale disturbance detection. Ecol Appl Publ Ecol Soc Am 17:235–250
Misra A (2013) Climate change impact, mitigation and adaptation strategies for agricultural and water resources, in Ganga Plain (India). Mitig Adapt Strateg Glob Chang 18:673–689
Natural Resources Conservation Service (NRCS) (1999) Soil taxonomy: a basic system of soil classification for making and interpreting soil surveys, 2nd ed. United States Department of Agriculture (USDA), Washington, p 871
Nawar S, Reda M, Farag F, El-nahry A (2011) Mapping soil salinity in El-Tina plain in Egypt using geostatistical approach. Geoinformatics Forum, Salzburg, pp 81–90
Nemani R, Running S (1997) Land cover characterization using multitemporal red, near-IR, and thermal-IR data from NOAA/AVHRR. Ecol Appl 7:79–90
North Sinai Governorate (2011) North Sinai (Arabic), El-Arish, Egypt, p 20
Othman AA, Rabeh SA, Fayez M et al (2012) El-Salam canal is a potential project reusing the Nile Delta drainage water for Sinai desert agriculture: Microbial and chemical water quality. J Adv Res 3:99–108
Peel MC, Finlayson BL, Mcmahon TA (2007) Updated world map of the Köppen-Geiger climate classification. Hydrol Earth Syst Sci 11:1633–1644
Pickett STA, White PS (1987) The ecology of natural disturbance and patch dynamics. Academic, New York, p 472
Rengasamy P (2006) World salinization with emphasis on Australia. J Exp Bot 57:1017–1023
Richards JA (2013) Remote sensing digital image analysis: an Introduction, 5th edn. Springer, Heidelberg, p 494
Salinas C, Mendieta J (2012a) The cost of mitigation strategies for agricultural adaptation to global change. Mitig Adapt Strateg Glob Chang :1–9. doi: 10.1007/s11027-012-9400-8
Salinas CX, Mendieta J (2012b) Effectiveness of the strategies to combat land degradation and drought. Mitig Adapt Strateg Glob Chang. doi:10.1007/s11027-012-9421-3
Salinas CX, Mendieta J (2012c) Mitigation and adaptation investments for desertification and climate change: an assessment of the socioeconomic return. Mitig Adapt Strateg Glob Chang. doi:10.1007/s11027-012-9380-8
Stiles D (1984) Desertification: the time for action. Environmentalist 4:93–96
Thomas DSG (2011) Arid environments: their nature and extent. Arid Zone Geomorphology. John Wiley & Sons, Ltd, pp 1–16
Tilman D (1985) The resource-ratio hypothesis of plant succession. Am Nat 125:827–852
U.S. Geological Survey (2011a) Vegetation indices monthly L3 global 1km. URL. https://lpdaac.usgs.gov/products/modis_products_table/mod13a3
U.S. Geological Survey (2011b) Surface reflectance 8-day L3 global 250m. URL. https://lpdaac.usgs.gov/products/modis_products_table/mod09Q1
U.S. Geological Survey (2011c) Global multi-resolution terrain elevation data 2010 (GMTED2010). URL. http://eros.usgs.gov/#/Find_Data/Products_and_Data_Available/GMTED2010
U.S. Salinity Laboratory (1954) Diagnosis and Improvement of saline and alkali soils, handbook 6. U.S. Government Printing Office, Washington, p 172
Wang XD, Zhong XH, Liu SZ et al (2008) Regional assessment of environmental vulnerability in the Tibetan Plateau: development and application of a new method. J Arid Environ 72:1929–1939
Weng Q (2002) Land use change analysis in the Zhujiang Delta of China using satellite remote sensing, GIS and stochastic modelling. J Environ Manage 64:273–284
WFP (2006) Country programme-Egypt (2007–2011). Rome, p25
World Bank (2013) Climate baseline. Egypt dashboard. URL. http://sdwebx.worldbank.org/climateportal/index.cfm?page=country_historical_climate&ThisRegion=Africa&ThisCCode=EGY
Yang J, Weisberg PJ, Bristow NA (2012) Landsat remote sensing approaches for monitoring long-term tree cover dynamics in semi-arid woodlands: comparison of vegetation indices and spectral mixture analysis. Remote Sens Environ 119:62–71
Zahran MA, Willis AJ (2009) The vegetation of Egypt, 2nd edn. Springer, Heidelberg, p 451
Zar JH (2010) Biostatistical analysis, 5th edn. Prentice Hall, New Jersey, p 960